



Bifunctional transalkylation and hydrodeoxygenation of anisole over a Pt/HBeta catalyst

Xinli Zhu, Lance L. Lobban, Richard G. Mallinson, Daniel E. Resasco*

Center for Biomass Refining, School of Chemical, Biological, and Materials Engineering, The University of Oklahoma, Norman, OK 73019, USA

ARTICLE INFO

Article history:

Received 1 December 2010

Revised 20 March 2011

Accepted 30 March 2011

Available online 19 May 2011

Keywords:

Bifunctional hydrodeoxygenation

Phenolic compound

Pt/HBeta

Anisole

Lignin

Hydrogenation

Hydrogenolysis

ABSTRACT

The catalytic conversion of anisole (methoxybenzene), a phenolic model compound representing a thermal conversion product of biomass lignin, to gasoline-range molecules has been investigated over a bifunctional Pt/HBeta catalyst at 400 °C and atmospheric pressure. The product distribution obtained on the bifunctional catalyst was compared with those obtained on monofunctional catalysts (HBeta and Pt/SiO₂). This comparison indicates that the acidic function (HBeta) catalyzes the methyl transfer reaction (transalkylation) from methoxyl to the phenolic ring, yielding phenol, cresols, and xylenols as the major products. The metal function catalyzes demethylation, hydrodeoxygenation, and hydrogenation in sequence, resulting in phenol, benzene, and cyclohexane. On the bifunctional catalyst, both methyl transfer and hydrodeoxygenation are achieved at significantly higher rates than over the monofunctional catalysts, leading to the formation of benzene, toluene, and xylenes with lower hydrogen consumption and a significant reduction in carbon losses, in comparison with the metal function alone. In addition, on the bifunctional Pt/HBeta, the rate of deactivation and coke deposition are moderately reduced.

© 2011 Elsevier Inc. All rights reserved.

1. Introduction

Production of liquid hydrocarbon fuels from abundant lignocellulosic biomass is being considered as a sustainable energy process. Upgrading bio-oil derived from biomass via fast pyrolysis into transportation fuels is an important step to accomplish this process. Lignin is a biopolymer formed from three main monomers: coumaryl alcohol, coniferyl alcohol, and sinapyl alcohol. In contrast to cellulose and hemicellulose, from which thermal processing produces high concentrations of relatively small oxygenates, lignin breaks down the polymer leading to high concentrations of phenolic molecules (phenol, guaiacol, syringol and their derivatives, see Scheme 1). Therefore, phenolic compounds represent a significant fraction of the biomass pyrolysis bio-oil [1–4] and remain a challenge for upgrading [3]. While building up the carbon chain is necessary for small oxygenates conversion, most phenolics are already in the gasoline range, but they require a deoxygenation process that should preserve the carbon number within the range of gasoline. As previously proposed [5], model compound studies are of crucial importance to establish the conditions for conversion of phenolic-rich streams.

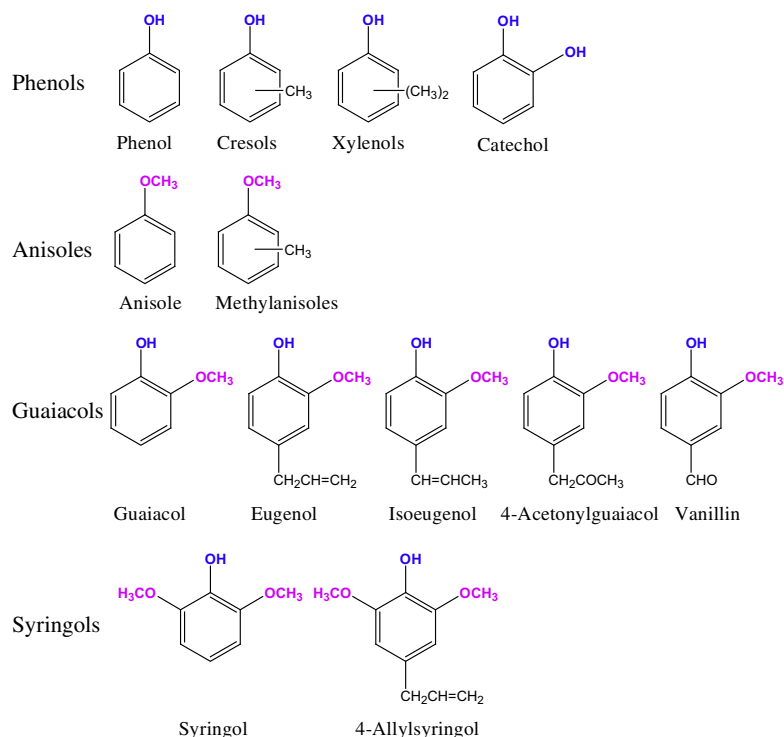
Hydrotreating and zeolite upgrading are the two main approaches for bio-oil conversion, and have been and are being intensively studied. High temperature (250–400 °C) and high pressure (3–5 MPa) hydrotreating of bio-oil over sulfided CoMo or NiMo

catalysts can effectively reduce the oxygen content of phenolics in the bio-oil [6–21]. However, this type of processing results in a significant loss of liquid yield, requires high hydrogen consumption, and produces a sulfur containing stream. Zeolite upgrading (including hydrocracking) is operated at atmospheric pressure and high temperatures (300–600 °C) with lower hydrogen consumption [22–28]. Though zeolites are effective in conversion of small oxygenates (such as aldehydes and ketones) through acid catalyzed reactions [22,29–31], their capability for deoxygenation of phenolics is limited [23–28]. Increasing attention has been paid to low temperature (<200 °C) and high pressure (3–5 MPa) hydrogenation processes [32–36]. Full hydrogenation of the phenolic ring over metal sites followed by dehydration and re-hydrogenation yields aliphatic hydrocarbons. It is evident that the hydrogen consumption is high in this process and the products are not as valuable for gasoline blending. Minimizing carbon loss and also hydrogen consumption (i.e. improving hydrogen efficiency [37]) are important parameters for the incorporation of biomass-derived liquids in refineries. Therefore, while the addition of aromatics to the gasoline and diesel fuel pools will still be limited by technical and legislative caps, production of aromatics from the lignin fraction of biomass is probably the most economically favorable process. Also, aromatics are important building blocks in petrochemical industry, and replacing their source from fossil to renewable sources is certainly advantageous.

As shown in Scheme 1, the hydroxyl (–OH) and methoxyl (–OCH₃) are the major functional groups of lignin derived phenolics. In previous work, it has been shown that the methyl

* Corresponding author. Fax: +1 405 325 5813.

E-mail address: resasco@ou.edu (D.E. Resasco).



Scheme 1. Structure of phenolic compounds.

in the methoxyl of phenolics could be transferred to the aromatic ring through acid catalyzed transalkylation reactions over HZSM-5; while the hydroxyl appears to be inert under the same reaction conditions [28]. In this work, high temperature and low (atmospheric) pressure operation for deoxygenation of phenolics over a bifunctional metal/zeolite catalyst are demonstrated. Moreover, this deoxygenation is accomplished with low carbon loss in the form of methane and low hydrogen consumption by phenolic ring hydrogenation. Anisole (methoxybenzene) has been chosen as a model compound of phenolics because (1) anisole contains an isolated methoxyl, one of the major functional groups of the lignin phenolics; (2) the analysis of product distribution is relatively simple, i.e., after removal of the methyl from the methoxy group, the hydroxyl group remains in the original molecule, while the source of any methyl transferred to another molecule can be accounted for; and (3) anisole is liquid at room temperature, no solvent is needed for feeding, and thus, the influence of solvent on both reaction and analysis is avoided. A well-known alkane isomerization catalyst, Pt/HBeta, has been chosen as a bifunctional catalyst to test, with the acid sites of HBeta catalyzing the alkyl transfer reaction [28] and Pt catalyzing the deoxygenation reaction. Anisole conversion over HBeta (acid zeolite function) and Pt/SiO₂ (metal function) is included for comparison.

2. Experimental

2.1. Catalyst preparation and characterization

The ammonium form of Beta zeolite (Zeolyst, CP814C, Si/Al = 19, $S_{\text{BET}} = 710 \text{ m}^2/\text{g}$) was calcined at 550 °C for 4 h to obtain HBeta. Pt/HBeta and Pt/SiO₂ catalysts were prepared by incipient wetness impregnation of HBeta and SiO₂ (HiSil 210, $S_{\text{BET}} = 135 \text{ m}^2/\text{g}$) with an aqueous solution of H₂PtCl₆·6H₂O (Aldrich) overnight and were then dried at 110 °C for 12 h, followed by calcination at 400 °C for 4 h.

The morphology of HBeta zeolite was studied by scanning electronic microscopy (SEM) on a Jeol JSM-880 electron microscope, equipped with energy dispersive X-ray analysis. Powder X-ray diffraction (XRD) patterns of the catalyst samples were obtained on a Bruker D8 Discover diffractometer. The acid density of the HBeta zeolite was determined by temperature programmed desorption (TPD) of isopropylamine (IPA) [38,39] following the procedure described previously [30]. The dispersion of Pt was estimated by dynamic pulse CO adsorption. Catalyst samples were reduced at 300 °C by flowing H₂ for 1 h, and the temperature was held at 300 °C for another 0.5 h in flowing He to desorb the adsorbed H₂. After the sample was cooled down to room temperature in He, 100 μL of 5% CO/He gas mixture was pulsed onto the sample until saturation of the surface of the catalyst was reached. The CO consumption was monitored by a thermal conductivity detector (TCD, SRI 310C GC). A CO/Pt stoichiometry of 1/1 was used to estimate the Pt dispersion. Transmission electron microscopy (TEM) images were obtained on a Jeol 2010F field emission system operated at 200 kV. A finely ground catalyst powder, pre-reduced at 300 °C for 1 h, was dispersed ultrasonically in ethanol and then deposited on a carbon coated copper grid for TEM measurement. The number-weighted (d_n) and the surface-weighted average particle size (d_s) were calculated using $d_n = \sum n_i d_i / \sum n_i$ and $d_s = \sum n_i d_i^3 / \sum n_i d_i^2$, respectively, where d_i is the particle size of n_i . Approximately 200 particles from images of different places of each sample were counted to calculate the d_n and d_s . The coke deposition was evaluated by temperature programmed oxidation of spent samples using 5% O₂/He with a Cirrus mass spectrometer (MS, MKS) detector. The temperature was ramped from room temperature to 900 °C with a heating rate of 10 °C/min. The quantification of carbon deposits was done by using calibrated pulses of CO₂ and CO.

2.2. Catalytic performance

Catalytic conversion of anisole was investigated in a fixed-bed quartz tube (6 mm o.d.) reactor at atmospheric pressure. The

catalyst sample (40–60 mesh) was reduced in flowing H_2 at 300 °C for 1 h, and then the temperature was raised to 400 °C for reaction. The anisole was fed using a syringe pump (kd scientific) and vaporized before entering the reactor. All lines were heated to avoid any condensation. The H_2 /Anisole molar ratio was kept at 50 in all runs. The products were quantified online in a gas chromatograph (GC 6890, Agilent), equipped with an Innowax capillary column (60 m) and a flame ionized detector (FID). The effluent was trapped by methanol in an ice-water bath and its components identified by GC-MS (Shimadzu QP2010s). A standard sample was injected for isomer identification.

To analyze the product evolution from differential to integral reactor conditions, the W/F was varied from 0 to 4 h, varying both catalyst amount (5–240 mg) and organic feed flow rate (0.03–0.48 mL/h). The W/F is defined as the ratio of catalyst mass (g) to organic feed flow rate (g/h). In a standard run with W/F of 0.5 h, the H_2 flow rate, anisole flow rate, and catalyst amount were 20 scm^3/min , 0.12 mL/h, and 60 mg, respectively. To determine whether the measurements were conducted in the absence of internal mass transfer limitations, the conventional Weisz–Prater criterion was employed. Similarly, to test for external mass transfer limitations, runs at varying gas velocities were compared. A fresh catalyst sample was used for each W/F , and the data with a time on stream (TOS) of 0.5 h were used for each W/F . The conversion and yield are reported in $Mol_{carbon}\%$. To test the effect of cofeeding water on anisole conversion, deionized water was fed with a parallel syringe pump keeping a H_2O /Anisole mass ratio of 1/4.

3. Results and discussion

3.1. Catalyst characterization

SEM observations of the HBeta zeolite show well ordered and uniform crystallites with a quasi-spherical shape, with sizes in the 0.5–1 μm range (see Fig. S1A). EDX elemental analysis (Fig. S1B) indicates that the Si/Al ratio is near 24. The characteristic BEA structure was the only phase identified by the XRD pattern in the Beta zeolite sample (Fig. S2). The IPA/TPD measured Brønsted acid density of HBeta was 0.665 mmol/g, in good agreement with the EDX measured Al content, but somewhat lower than that calculated from the Si/Al ratio specified by the manufacturer (i.e., 19, instead of the measured 24). Also, the good agreement between the measured density of Brønsted sites and the total density of Al ions indicates that most of the Al are forming Brønsted sites.

Table 1

Pt particle sizes estimated from XRD, TEM, and CO chemisorption.

Sample	XRD	TEM		CO chemisorption	
	d_{XRD} (nm)	d_H (nm)	d_S (nm)	D_{CO} (%)	d_{CO}^a (nm)
1% Pt/SiO ₂	7.1	4.1	8.3	20	5.5
1% Pt/HBeta	–	1.6	2.4	71	1.6
0.2% Pt/HBeta	–	1.4	1.6	78	1.4

^a Pt particle size was estimated using $d_{CO} = 1.1/D_{CO}$, where D_{CO} is the Pt dispersion measured from CO chemisorption.

The XRD patterns of the Pt/SiO₂ sample (Fig. S2) revealed the presence of FCC Pt, superimposed to a broad feature produced by the amorphous structure of SiO₂. The estimated Pt particle size from the full width at half maxima, using the Sherrer equation, was 7.1 nm. By contrast, no Pt diffraction peaks were observed with the Pt/HBeta samples (Fig. S2), indicating a high dispersion of Pt on HBeta zeolite, i.e., particle size <5 nm.

Representative TEM images of 1% Pt/SiO₂ and 1% Pt/HBeta are displayed in Fig. 1, which include Pt particle size distributions as insets. Although most of the Pt particles in the Pt/SiO₂ samples had sizes in the range of 2–4 nm, larger particles up to 20 nm in diameter were occasionally observed. A much narrower Pt particle size distribution was obtained over 1% Pt/HBeta, with most of the particles in the 1–2 nm range. The Pt particle size distribution was even narrower for the Pt/HBeta of lower Pt loading (0.2 wt.%) (Fig. S3). It is expected that Pt particles smaller than 1 nm may reside inside the zeolite micropores.

The Pt dispersions (CO/Pt) estimated from CO uptakes were 0.2, 0.7, and 0.8, for 1% Pt/SiO₂, 1% Pt/HBeta, and 0.2% Pt/HBeta catalysts, respectively. As shown in Table 1, the estimated Pt particle sizes from these CO chemisorption values are in good agreement with those estimated from XRD and TEM, confirming that significantly higher Pt dispersion is achieved over zeolite Beta than over SiO₂. As anticipated, the sizes derived from CO chemisorption are consistently smaller than those derived from TEM and XRD, since the chemisorption values weight more heavily the smallest particles, which may not be easily detected by TEM or XRD.

3.2. Anisole conversion over HBeta

The conversion of anisole was first studied over the acidic zeolite. HBeta was chosen in this work for phenolics conversion, since zeolite Beta has a three-dimensional 12-member ring pore

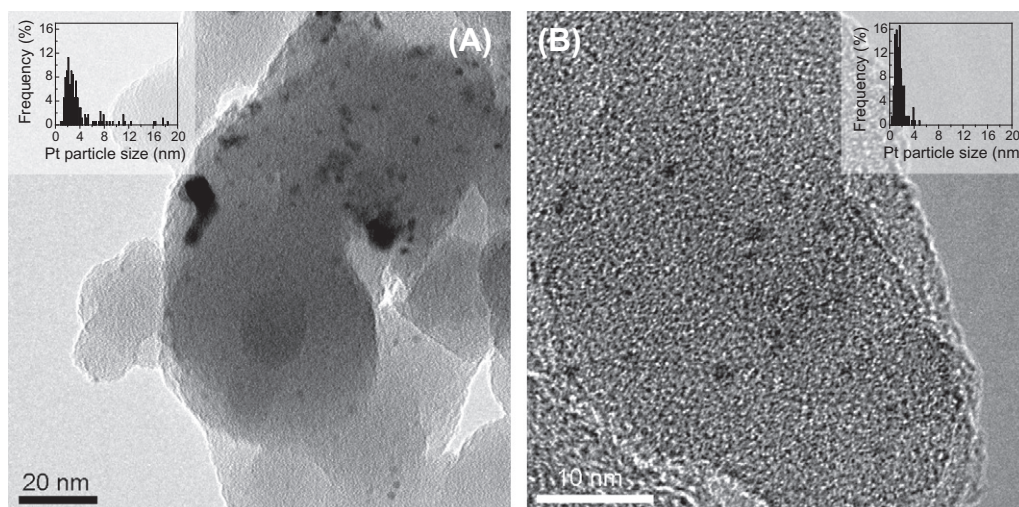


Fig. 1. TEM images of (A) 1% Pt/SiO₂ and (B) 1% Pt/HBeta; insets: Pt particle size distribution. Both samples were reduced at 300 °C for 1 h, passivated, and brought to the TEM minimizing exposure to ambient air.

structure that is able to accommodate relatively large phenolic compounds better than 10-number ring zeolites, such as ZSM-5. As shown in Fig. 2, total conversion of anisole is achieved at W/F of 0.33 h (Fig. 2A). At low W/F , the major products are phenol (Ph) and methylanisole (MA), which are obtained in equal yields (Fig. 2B), indicating that the first step of anisole conversion is a disproportionation reaction. As we have previously indicated [28], while this step is kinetically described as a bimolecular step, it does not necessarily occur bimolecularly at the elementary step level. It is possible that in the first step the methoxy group decomposes on an acid site, while the methyl group is readily accepted by another molecule in a subsequent step.

Increasing W/F leads to the consumption of MA and the production of cresol isomers (Cr), xylenol isomers (Xol), and trimethylphenol isomers (which is included in xylenols due to poor separation). Similar to the behavior observed over HZSM-5 [28], a number of transalkylation reactions (major paths), intramolecular rearrangements, and dealkylation reactions (minor paths) were observed over the HBeta zeolite.

As shown in Fig. 2C, the minor products consisted of aliphatic hydrocarbons (C_{1-9}), aromatics (benzene, toluene, xylenes), dimethylanisole (DMA) isomers, and heavies (naphthalene, multiple methylated benzenes). The low yields (<3%) of these minor products imply that the demethylation and deoxygenation reactions occur only to a limited extent. It must be noted that the yield of dimethylanisoles is maximum at intermediate W/F , suggesting that they are intermediates in the formation of xylenols. As summarized in Fig. 2D, the main reaction catalyzed by the acidic function is the methyl transfer from the methoxyl to the phenolic rings, which include phenol, cresol, methylanisoles, finally forming the major products of phenol, cresols, and xylenols.

3.3. Anisole conversion over Pt/SiO₂

A Pt/SiO₂ catalyst was employed to examine the behavior of the metal function during anisole conversion. Even at the maximum temperature and space time tested (400 °C, $W/F = 4$ h), the conversion of anisole over the bare support was less than 2%, confirming that SiO₂ is inactive for this reaction. As shown in Fig. 3, total conversion of anisole was achieved over Pt/SiO₂ at a W/F of 1 h, while complete deoxygenation was only obtained at a much higher W/F (about 4 h). At low W/F , the rates of phenol (Ph) and methane (CH₄) production were very high, while those for other products were nearly zero, indicating that, over Pt, demethylation of anisole is the primary reaction. Contrary to the case on the acidic zeolites, the decomposed methyl group does not remain on the surface nor is it transferred to another molecule, but it is rapidly hydrogenated to form methane. Similar behavior has been observed in the anisole conversion over CoMo and NiMo catalysts [7,9].

At intermediate W/F , the benzene (Ben) yield increases at the expense of phenol, indicating the involvement of the direct hydrodeoxygenation reaction. Further increase in W/F leads to the partial hydrogenation of benzene to cyclohexane and further converted to other aliphatic hydrocarbons. At this high temperature (400 °C), the extent of aromatic hydrogenation is limited by equilibrium. The major reaction pathway is summarized in Fig. 3C.

Two alternative pathways have been proposed in the literature to describe the deoxygenation of phenolics: (1) direct hydrodeoxygenation forming aromatics and water; (2) hydrogenation of the phenolic ring followed by dehydration forming a double bond in the ring (cyclohexene derivative) and re-hydrogenation of the double bond to cyclohexane derivatives [10]. The catalyst type and reaction conditions play an important role on the reaction

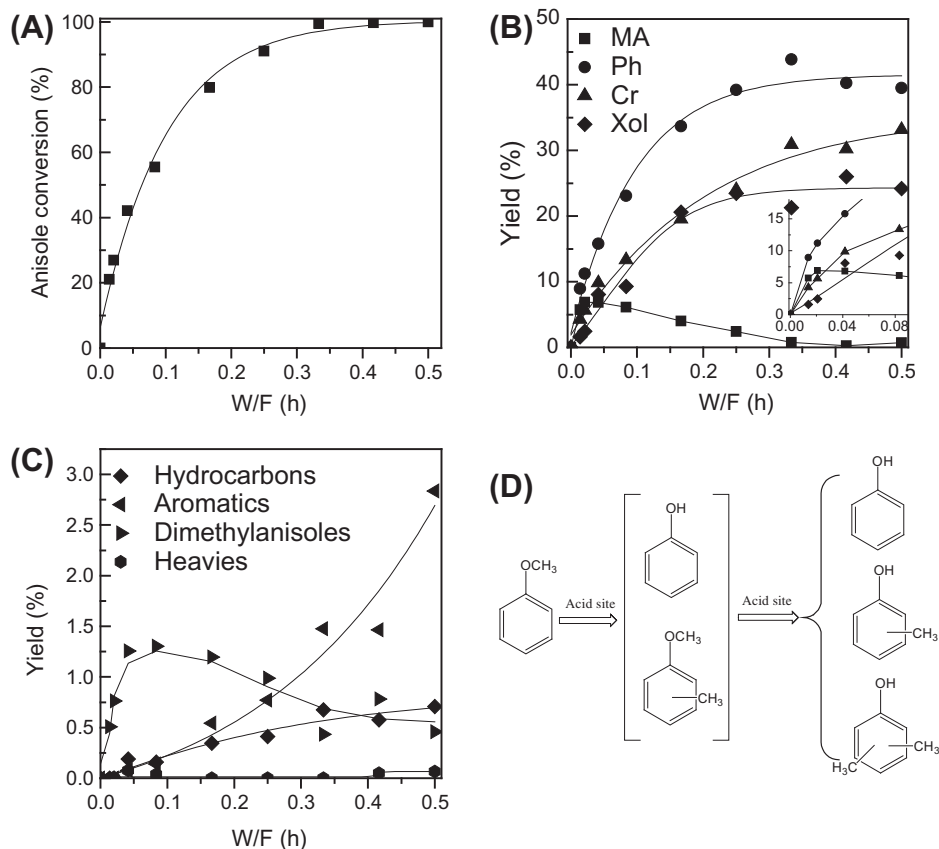


Fig. 2. Anisole conversion over HBeta: Effect of W/F on (A) anisole conversion; (B) major product distributions; (C) minor product distributions; and (D) major reaction pathway. Reaction conditions: $T = 400$ °C, $P = 1$ atm, $H_2/\text{Anisole} = 50$, TOS = 0.5 h for each W/F . The inset shows the distribution of products at very low W/F .

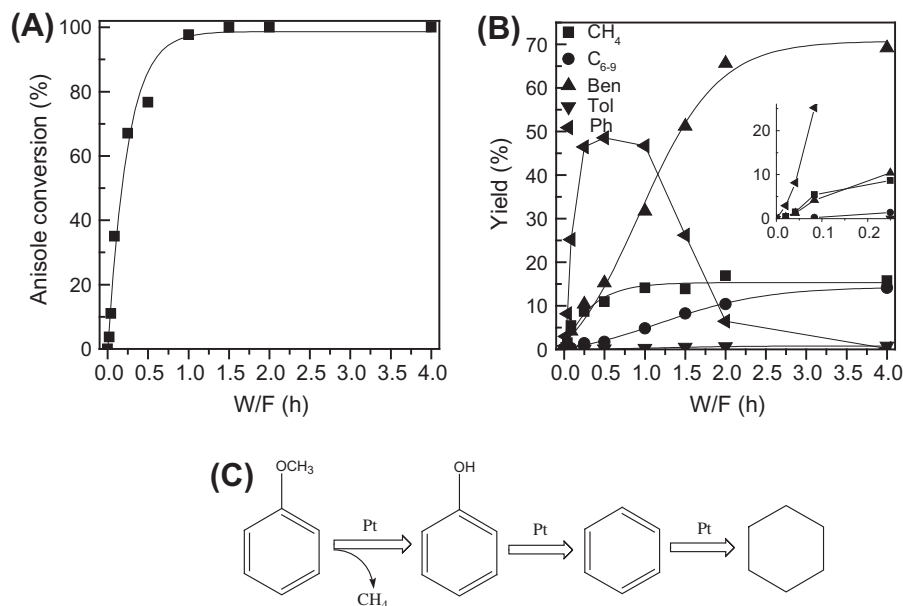


Fig. 3. Anisole conversion over 1% Pt/SiO₂: Effect of W/F on (A) anisole conversion; (B) product distribution; and (C) major reaction pathway. Reaction conditions: $T = 400$ °C, $P = 1$ atm, $H_2/\text{Anisole} = 50$, TOS = 0.5 h for each W/F. The inset shows the distribution of products at very low W/F.

pathways [8,10,12–14,16,18,20]. For example, while on sulfided NiMo catalyst hydrogenation followed by dehydration seems to be the preferred path, direct hydrodeoxygenation has been proposed to be the major path for a sulfided CoMo catalyst [8,20]. Increased H₂S partial pressures decrease the surface concentration of coordinative unsaturated sites and shifts the reaction pathway to the hydrogenation/dehydration route [13,16,18].

The product distribution observed in this work for the Pt/SiO₂ catalyst shows that the direct hydrodeoxygenation reaction is the dominant reaction under our current operating conditions. However, one cannot expect a direct hydrogenolysis of the C_{aromatic}–OH bond. In fact, theoretical calculations show that the bond strength of C_{aromatic}–OH bond (e.g., phenol) is 84 kJ/mol higher than that of the C_{aliphatic}–OH (e.g., aliphatic alcohols) [6]. This significant difference in bond strength is due to the delocalization of the out of plane lone pair orbital of oxygen onto the π orbital of the phenolic ring. In addition, formation of a surface intermediate that would bind both C and O to the surface would require a sp²–sp³ transformation that is not favored if the aromatic ring remains intact. Thus, the apparent direct hydrodeoxygenation may involve a partial hydrogenation of the phenolic ring near the C_{aromatic}–OH bond, resulting in the temporary removal of the delocalization effect followed by rapid dehydration. The result would be the formation of benzene and water. A similar reaction pathway has been proposed for deoxygenation of phenol on CoMo catalysts [19] and hydrogenation of cresol on Rh catalysts [40].

3.4. Anisole conversion over Pt/HBeta

As shown in Fig. 4, complete conversion of anisole over Pt/HBeta was achieved at a W/F of 0.1 h, which is 10 times shorter than that required to reach the same conversion over Pt/SiO₂. At low conversions, the products obtained on Pt/HBeta are similar to those observed with the HBeta catalyst, which include methylanisole (MA), phenol (Ph), cresol isomers (Cr), xylenol isomers (Xol), and dimethylanisole isomers (DMA). However, above a given conversion level, these oxygenates start being converted into aromatic hydrocarbons, benzene (Ben), toluene (Tol), xylene isomers (Xy), and C₉₊ aromatics (Fig. 4C). At a W/F of about 0.3 h, the oxygenated

aromatics have been completely converted. It is interesting to note that almost no aromatics saturation was observed when full deoxygenation was achieved over Pt/HBeta catalysts. In contrast, in a recent study of the conversion of phenol over Pt/HY catalyst [34], mostly saturated rings were observed in the product. The differences in the results from that study with the current contribution may be ascribed to their higher pressures and lower temperatures (4 MPa and 200 °C), which are more conducive to ring saturation. This is an interesting point for selecting a given process strategy; since dehydrogenation/hydrogenation are significantly faster reactions than deoxygenation, they are usually pseudo-equilibrated and therefore the combination of appropriate temperature and pressure conditions can be used to tailor the naphthenic/aromatic ratio, depending on the desired product.

It is apparent that the simultaneous presence of the two catalytic functions greatly enhances the deoxygenation. This enhancement could be not only due to the independent contributions of the Brønsted sites (methyl transfer reaction) and the metal sites (hydrodeoxygenation), but also to a synergistic bifunctional path, as discussed later.

Fig. 5 compares the yield of the major products at the same overall conversion of anisole (~80%) over HBeta, Pt/HBeta, and Pt/SiO₂. To illustrate the influence of Pt in the acid-catalyzed alkyl transfer, the deoxygenated products (Ben, Tol, Xy) are added together with their corresponding oxygenates (Ph, Cr/DMA, and Xol/DMA). Thus, the effect of deoxygenation on product distribution is eliminated for comparison purposes. A clear trend is obvious among the three catalysts. At the same anisole conversion, the yield of C₆ aromatics (Ben + Ph) is highest over Pt/SiO₂ and gradually decreases for Pt/HBeta and HBeta. By contrast, no C₇ or C₈ aromatics are observed for Pt/SiO₂, while they are significant for Pt/HBeta and, more so, for HBeta. These results clearly show that Pt alone only catalyzes demethylation, and it interferes in the transalkylation process when it is simultaneously present with the Brønsted sites responsible for this reaction. It is apparent that some methyl groups left on the surface from the demethylation of anisole are hydrogenated over Pt, yielding CH₄ instead of transalkylating to another aromatic. This conclusion is supported by the observed CH₄ yields, which over Pt/HBeta are higher than over HBeta, but significantly lower than over Pt/SiO₂.

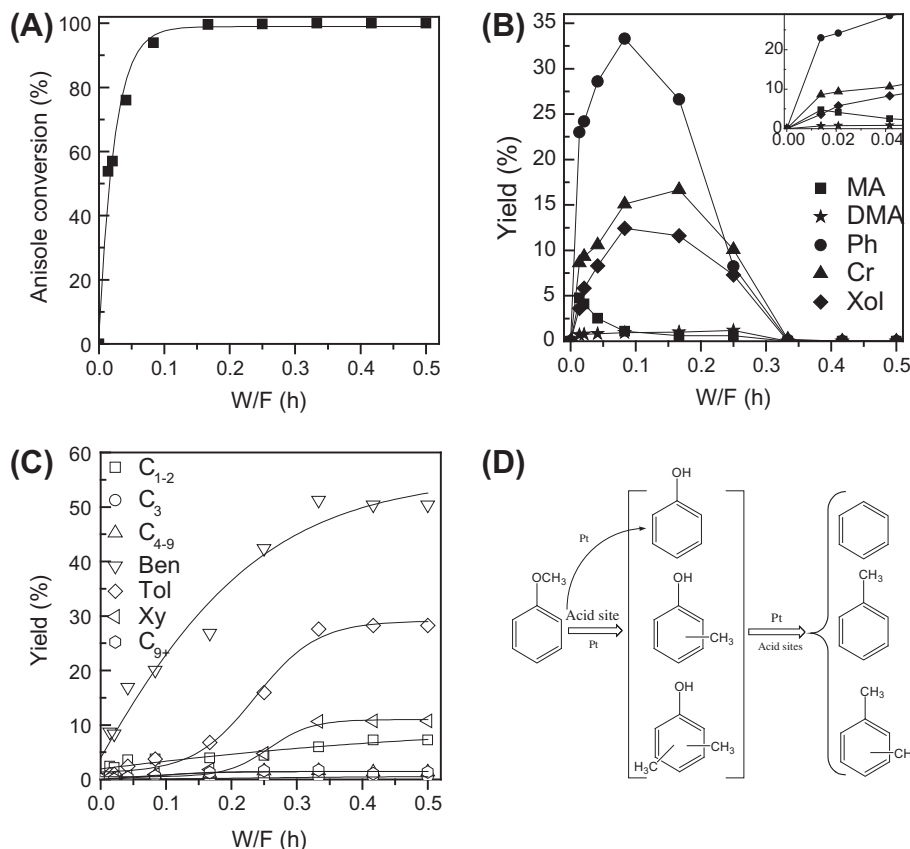


Fig. 4. Anisole conversion over 1% Pt/HBeta: Effect of W/F on (A) anisole conversion; (B) oxygenate distributions; (C) hydrocarbon distributions; and (D) major reaction pathway. Reaction conditions: $T = 400\text{ }^{\circ}\text{C}$, $P = 1\text{ atm}$, $\text{H}_2/\text{Anisole} = 50$, $\text{TOS} = 0.5\text{ h}$ for each W/F. The inset shows the distribution of products at very low W/F.

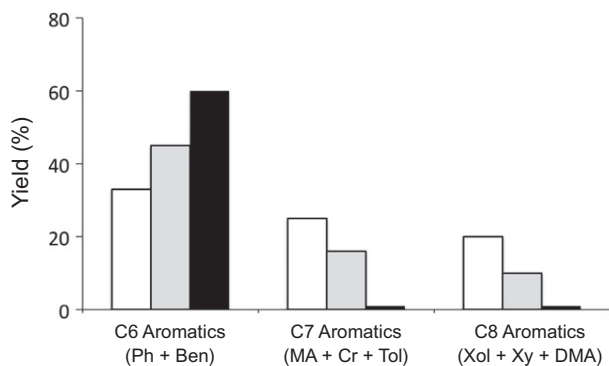


Fig. 5. Yield of different C-number oxygenated and deoxygenated aromatics, at similar anisole conversion ($\sim 80\%$) over the different catalysts. Open bar: HBeta; shaded bar: Pt/HBeta; solid bar: Pt/SiO₂.

An important result that requires further analysis is the enhanced conversion of anisole observed on the Pt/HBeta catalyst. For instance, as shown in Table 2, to achieve a given anisole conversion (e.g. 30%), the W/F required over Pt/HBeta (0.008 h) is only a third of that required over HBeta (0.027 h). At this relatively low conversion, most of the anisole consumed is involved in demethylation and transalkylation. The enhanced activity observed in the presence of Pt indicates that the metal accelerates the cleavage of the methoxy group (O–CH₃) in anisole. As previously discussed in our recent study on HZSM-5 [28], this is the first step in the reaction and an enhancement in the rate of the O–CH₃ bond breaking

Table 2

W/F for catalyst to achieve 30% total anisole conversion and 30% deoxygenation, and turn over frequency (TOF) for deoxygenation.

Sample	W/F (h)		TOF ^b (s ⁻¹)
	30% Conversion	30% Deoxygenation ^a	
HBeta	0.027		
1% Pt/SiO ₂	0.079	0.90	0.104
1% Pt/HBeta	0.008	0.12	0.330

^a Benzene, toluene, xylenes, and C₉₊ aromatics are considered as deoxygenation products.

^b TOF is defined as moles of anisole conversion to deoxygenation products over per mole surface Pt per second. The TOF is obtained from anisole conversion to deoxygenation products less than 10% by adjusting W/F. The Pt dispersion estimated from CO chemisorption was used for TOF.

enhances the overall reaction rate. For example, it was shown in the previous study that addition of water improves the overall reaction rate by a factor of 2.5 due to the acceleration of O–CH₃ bond cleavage via hydrolysis over Brønsted acid sites by H₂O [28].

What is even more remarkable is that the rate of anisole consumption on Pt/HBeta is even higher than on Pt/SiO₂. However, the evolution of methane is much lower on the former than on the latter. This result indicates that the methyl groups that are produced by demethylation on Pt are effectively transferred to other aromatics. This transfer does not occur on Pt alone (see Fig. 5); therefore, these should necessarily involve the participation of the Brønsted sites in a synergistic phenomenon that can only occur when Pt is in intimate contact with the Brønsted site.

At the same time, a synergistic effect is observed for deoxygenation, which is a metal-catalyzed reaction. As shown in Table 2,

achieving 30% deoxygenation of the oxygenated aromatics over Pt/SiO₂ requires a W/F seven times greater than that required over the Pt/HBeta catalyst having the same Pt loading. To further quantify the difference in specific deoxygenation rates over the two catalysts, the turn over frequency (TOF) was calculated using the data obtained under differential reaction conditions with a deoxygenation conversion lower than 10%. As shown in Table 2, the TOF over Pt/HBeta was three times higher than that over Pt/SiO₂, which suggests that the zeolite environment plays an important role in enhancing the deoxygenation activity of Pt.

One can speculate that a Brønsted acid site adjacent to a Pt particle could facilitate the deoxygenation reaction by protonating the oxygen in phenol, which would inhibit the delocalization of the O lone pair orbital with the aromatic π orbital and thus would facilitate the Pt-catalyzed partial hydrogenation of aromatic ring at the bond close to the C_{aromatic}-OH. With this partial hydrogenation, the electron delocalization is removed and water elimination can readily happen over the adjacent Brønsted acid site. Due to the high temperatures used in this study, the formation of aromatics is favored, so partially hydrogenated products are not observed.

In summary, addition of Pt to HBeta has a synergistic effect on activity (Fig. 4D). In the first place, Pt accelerates the rate of alkyl transfer from the methoxy group to the phenolic ring catalyzed by Brønsted acid sites. At the same time, the Brønsted acid sites adjacent to Pt accelerate the hydrodeoxygenation rate occurring in a bifunctional reaction.

The Pt/HBeta catalyst exhibits a unique advantage for the conversion of aromatics containing a methoxy group compared with any other deoxygenation catalyst, in which carbon loss is unavoidable. That is, in the low temperature hydrolysis process catalyzed by acid sites, the methyl of the methoxy group is eliminated as methanol [32,33]; in the high temperature hydrotreating processes over sulfided catalysts or the Pt/SiO₂ catalyst studied here, carbon is lost as CH₄ [7,9,12,14,16,18,41]. In contrast, over the bifunctional Pt/HBeta catalyst, most of methyl is transferred to the phenolic ring and retained after deoxygenation, minimizing carbon loss.

Since alkylated aromatics are more attractive than benzene for fuel applications, and to further limit the carbon losses, a Pt/HBeta with reduced metallic function was tested. As shown in Table 3, when a 0.2% Pt/HBeta catalyst was used, five times longer W/F was needed to achieve full deoxygenation of anisole than over the 1% Pt/HBeta. However, a noticeable increase in toluene, xylenes, and C₉₊ aromatics at the expense of benzene was observed, indicating a decreased loss of carbon as CH₄. This result indicates that adjusting the metal/acid balance, one could control product distribution and improve liquid yield in the upgrading of bio-oils containing phenolics.

Table 3

Major product distributions for complete conversion of anisole over HBeta and complete deoxygenation of anisole over Pt/SiO₂ and Pt/HBeta catalysts.

Catalyst	HBeta	1% Pt/SiO ₂	1% Pt/HBeta	0.2% Pt/HBeta
W/F (h)	0.5	4	0.33	1.5
<i>Major product yield (%)</i>				
Phenol	39.5	0.2	0.1	0.7
Cresols	33.5	0	0.2	0.6
Xylenols	24.2	0	0	0.3
C ₁₋₂	0.2	15.4 ^a	6.0	4.2
C ₃	0.2	0	0.4	0.7
C ₄₋₉	0.2	14.1	1.6	1.5
Benzene	0.1	69.2	51.2	40.2
Toluene	0.1	0.8	27.6	31.8
Xylenes	0.3	0	10.6	14.4
C ₉₊ aromatics	0.3	0	1.7	3.4

^a CH₄ is the only product for C₁₋₂ aliphatic hydrocarbons.

3.5. Stability test and coke analysis

Fig. 6 shows the stability tests of the HBeta, 1% Pt/HBeta, and 1% Pt/SiO₂ catalysts during the anisole conversion runs. The W/F was adjusted to obtain a comparable initial conversion level over the three different catalysts. A more rapid deactivation was observed on HBeta than on either Pt/SiO₂ or Pt/HBeta, indicating that Pt plays a role in cleaning adjacent acid sites by hydrogenation of coke precursors. Also, SiO₂ being an inert support does not adsorb coke precursors as strongly as the acidic zeolite [42].

Deactivation of the catalyst with time on stream reduces the degree of deoxygenation, even when the anisole conversion is still 100%. Fig. 7 shows the effect of reaction time on the distribution of major products obtained over 1% Pt/HBeta at anisole conversions significantly lower than 100%. In this case, it is seen that catalyst deactivation causes the reduction in both hydrodeoxygenation and transalkylation reactions, resulting in decreases in yields of both deoxygenation products (Ben, Tol, Xy, and C₉₊ aromatics) and transalkylation products (Ph, Cr, Xol) except MA, which increases as catalyst deactivates, since MA is both a primary and an intermediate product for transalkylation.

It seems that deactivation affects hydrodeoxygenations more strongly than transalkylation, as evidenced by the decrease in

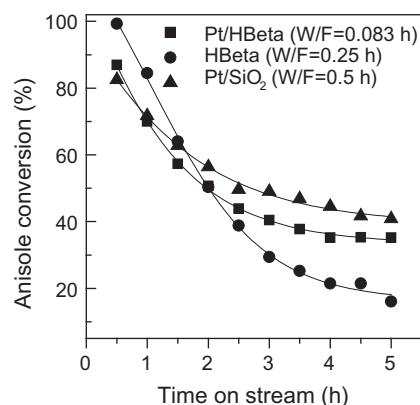


Fig. 6. Effect of time on stream on anisole conversion over HBeta, 1% Pt/SiO₂, and 1% Pt/HBeta catalysts. Reaction conditions: $T = 400\text{ }^{\circ}\text{C}$, $P = 1\text{ atm}$, $\text{H}_2/\text{Anisole} = 50$. The W/F was adjusted for each catalyst in order to achieve similar initial conversion.

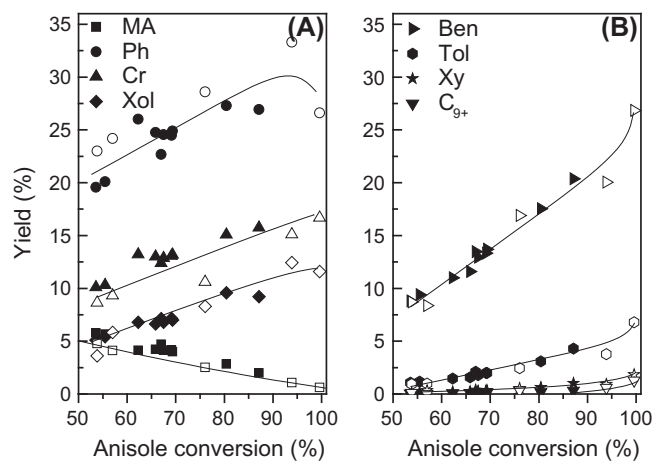


Fig. 7. Product yield as a function of overall anisole conversion over 1% Pt/HBeta. Different conversions were achieved by catalyst deactivation (solid symbols) and by varying W/F (open symbols). (A) Oxygenates and (B) aromatics. The reaction conditions for deactivation were the same as Fig. 6; the data for the W/F series are reproduced from Fig. 4, with anisole conversions lower than 100%.

selectivity to deoxygenated aromatics as the catalyst deactivates (Fig. 8). However, this difference is mostly due to the sequence of reactions. Transalkylation steps are involved in the primary reactions, while all hydrodeoxygenation steps occur in secondary reactions. Therefore, as the overall conversion drops, the latter are more affected. As a result, a decrease in selectivity to deoxygenated aromatics is clearly observed as the catalyst deactivates (Fig. 8). Therefore, when comparing two different catalysts, the comparison must be made at the same level of anisole conversion. For instance, it is seen that, at the same overall conversion, the selectivity to deoxygenation is much higher over Pt/HBeta than over Pt/SiO₂, confirming that Pt/HBeta is more effective for hydrodeoxygenation.

It is interesting to note that when changing conversion level over Pt/HBeta by either catalyst deactivation or by varying W/F (Fig. 7), the yields of all the major products fall near the same trend line when they are plotted as a function of anisole conversion, indicating that deactivation only reduces numbers of active sites without altering the chemistry. A type of deactivation that would show this behavior is pore blocking. This behavior is in line with a uniform distribution of Pt throughout the HBeta zeolite; otherwise, the metal/acid balance would be altered when pore blockage occurs.

Quantification of the carbon deposited during anisole conversion was accomplished by TPO of the spent catalysts. As shown in Fig. 9, a broad CO₂ evolution peak centered at 636 °C was observed for the HBeta catalyst. In contrast, two smaller peaks centered at 183 and 522 °C were observed over Pt/SiO₂. Addition of Pt to HBeta resulted in shift and a reduction in size of the intense peak observed for HBeta resulting in three peaks at around to 332, 507, and 569 °C. These shifts could be due to the presence of Pt that catalyzes the oxidation of coke, lowering the oxidation temperature significantly. The percentage of coke formed over Pt/HBeta was slightly reduced compared with that over the HBeta, but was significantly higher than that over Pt/SiO₂ (Table 4), suggesting that the extent of coke deposition is not only dependent on the presence or absence of Pt, but also on the acidity and pore structure of the support. However, when the amount of coke deposited was compared on the basis of converted anisole (Table 4), the ratios obtained over Pt/SiO₂ and Pt/HBeta were comparable, but significantly lower than the one over HBeta. In addition to the expected conclusion that Pt improves the coke tolerance, these results generate another interesting implication. That is, the products of anisole conversion (e.g. phenol, cresol) may be responsible for deactivation.

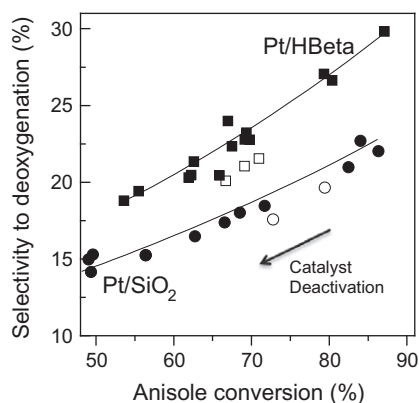


Fig. 8. Effect of deactivation on selectivity to deoxygenation during anisole conversion over 1% Pt/HBeta and 1% Pt/SiO₂. The reaction conditions were the same as those in Fig. 6. Solid symbol, without water; open symbol, with water (H₂O/An molar ratio = 1.5).

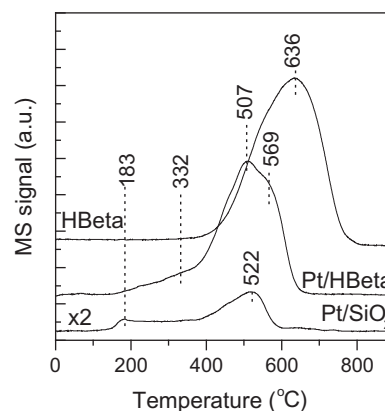


Fig. 9. Temperature programmed oxidation profiles of spent catalysts after 5 h on stream. Reaction conditions were the same as those in Fig. 6 for each catalyst.

Table 4

Coke formation over HBeta, 1% Pt/HBeta, 1% Pt/SiO₂ after 5 h reaction.^a

Catalyst	Coke formation	
	$g_{\text{carbon}}/g_{\text{catalyst}}$ (%)	$g_{\text{carbon}}/g_{\text{converted anisole}}$ (%)
HBeta	12.0	13.4
Pt/HBeta	10.2	3.2
Pt/SiO ₂	1.6	3.0

^a Reaction conditions were the same in Fig. 6 for each catalyst.

As in most studies dealing with upgrading of phenolics, deactivation is a crucial effect. Future commercial applications of lignin biomass conversion will require catalysts with improved resistance to deactivation. Improved catalysts might involve special preparations such as introducing mesopores inside the zeolite crystallite [30], improving metal dispersion through anchoring, adding effective promoters, optimizing the metal/acid balance inside the zeolite micropores. Alternatively, or in parallel, reactor engineering may also be needed to implement continuous catalyst regeneration.

The effect of water addition on anisole conversion was briefly studied since significant amounts of water are always present in bio-oil. These experiments were carried out under the same conditions as those shown in Fig. 6, except that between 2 and 3.5 h on stream, H₂O was fed to the reactor (Fig. 10). Remarkably, the addition of water caused an immediate enhancement in anisole conversion. It is believed that the addition of H₂O helps hydrolyzing the O–CH₃ bond of the methoxy group in anisole [28]. The observed improvement is more pronounced over the zeolite-based catalysts than over Pt/SiO₂, implying that the acid site may be more effective in catalyzing hydrolysis than Pt alone.

When the flow of water was interrupted after 3.5 h, the anisole conversion over HBeta dropped immediately to the level observed in the absence of water (Fig. 6). This behavior is similar to that previously observed for anisole conversion over HZSM-5 [28] and confirms that addition of water only enhances the anisole conversion rate, without affecting the rate of coke formation. In contrast, on the supported Pt catalysts, anisole conversion dropped much more slowly to the level of the dry run (Fig. 6), and it remained somewhat higher than in the dry run, even after 5 h. These results would indicate that, in the presence of Pt, water may help clean the surface to some extent.

It was also observed that the presence of water had only a small effect on the distribution of the major products as a function of anisole conversion. To make a direct comparison, the results of the water-containing runs have been included in Fig. 8 together with

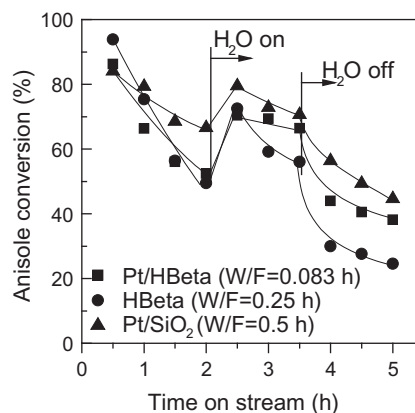


Fig. 10. Effect of water addition on anisole conversion over HBeta, 1% Pt/HBeta, and 1% Pt/SiO₂ catalysts. Reaction conditions: $T = 400\text{ }^{\circ}\text{C}$, $P = 1\text{ atm}$, $\text{H}_2/\text{Anisole molar} = 50$ at all times, $\text{H}_2\text{O}/\text{An molar} = 1.5$ (water started being injected at TOS = 2 h and stopped at TOS = 3.5 h).

those of the dry runs. The relatively minor differences in product distribution indicate that, in the presence of water, the deoxygenation reactions are somewhat inhibited, which would indicate that the enhancement of the anisole conversion by hydrolysis (acid-catalyzed primary reaction) is not accompanied by a comparable enhancement in the (metal catalyzed) secondary reaction.

4. Conclusions

Bifunctional catalytic hydrodeoxygenation of anisole to benzene, toluene, and xylenes has been demonstrated at $400\text{ }^{\circ}\text{C}$ and atmospheric pressure. Brønsted acid sites in HBeta catalyze the methyl transfer reactions from methoxyl to the phenolic ring. Metallic Pt only catalyzes demethylation, hydrodeoxygenation, and hydrogenation reactions, sequentially. Addition of Pt to the zeolite accelerates both methyl transfer reactions and hydrodeoxygenation reactions, with low hydrogen consumption and low carbon losses as methane. The presence of the metal improves the rate of cleavage of O–CH₃ and thus synergistically improves the overall rate of Brønsted acid catalyzed methyl transfer reactions. This may be interpreted as being due to a partial hydrogenation of the phenolic ring near the C_{aromatic}–OH bond on Pt that removes the delocalization of the out of plane O lone pair orbital with the phenolic ring π bond orbital, followed by rapid dehydration over an adjacent Brønsted acid site, re-forming the double bond and, therefore, the aromatic system.

In addition, the addition of metal to the acidic zeolite improves the stability of the catalyst with a moderate reduction in coke formation. Further optimization of the properties of metal/zeolite systems might lead to an effective catalyst for the hydrodeoxygenation of phenolics-rich bio-oils.

Acknowledgements

Financial support from the National Science Foundation EPSCOR (0814361), the Department of Energy (DE-FG36G088064), and the

Oklahoma Bioenergy Center is greatly appreciated. The authors thank Gregory W. Strout and Preston Larson for their help with TEM and SEM measurements, respectively.

Appendix A. Supplementary material

Supplementary data associated with this article can be found, in the online version, at doi:10.1016/j.jcat.2011.03.030.

References

- [1] D. Mohan, C.U.P. Pittman Jr., P.H. Steele, *Energy Fuels* 20 (2006) 848.
- [2] G.W. Huber, S. Iborra, A. Corma, *Chem. Rev.* 106 (2006) 4044–4098.
- [3] S. Crossley, J. Faria, M. Shen, D.E. Resasco, *Science* 327 (2010) 68–72.
- [4] J. Jae, G.A. Tompsett, Y.C. Lin, T.R. Carlson, J.C. Shen, T.Y. Zhang, B. Yang, C.E. Wyman, W.C. Conner, G.W. Huber, *Energy Environ. Sci.* 3 (2010) 358–365.
- [5] D.E. Resasco, S. Crossley, *AIChE J.* 55 (2009) 1082–1086.
- [6] E. Furimsky, *Appl. Catal. A* 199 (2000) 147–190.
- [7] J.B. Bredenberg, M. Huuska, J. Rätty, M. Korpio, *J. Catal.* 77 (1982) 242–247.
- [8] H. Weigold, *Fuel* 61 (1982) 1021–1026.
- [9] S.J. Hurff, M.T. Klein, *Ind. Eng. Chem. Fund.* 22 (1983) 426–430.
- [10] E.O. Odeunmi, D.F. Ollis, *J. Catal.* 80 (1983) 56–64.
- [11] D.C. Elliott, *Energy Fuels* 21 (2007) 1792–1815.
- [12] R.K.M.R. Kallury, W.M. Restivo, T.T. Tidwell, D.G.B. Boocock, A. Crimi, J. Douglas, *J. Catal.* 96 (1985) 535–543.
- [13] B.S. Gevert, J.E. Otterstedt, F.E. Massoth, *Appl. Catal.* 31 (1987) 119–131.
- [14] E. Laurent, B. Delmon, *Appl. Catal. A* 109 (1994) 77–96.
- [15] S.B. Gevert, M. Eriksson, P. Eriksson, F.E. Massoth, *Appl. Catal. A* 117 (1994) 151–162.
- [16] T.R. Viljava, R.S. Komulainen, A.O.I. Krause, *Catal. Today* 60 (2000) 83–92.
- [17] T.R. Viljava, E.R.M. Saari, A.O.I. Krause, *Appl. Catal. A* 209 (2001) 33–43.
- [18] M. Ferrari, R. Maggi, B. Delmon, P. Grange, *J. Catal.* 198 (2001) 47–55.
- [19] F.E. Massoth, P. Politzer, M.C. Concha, J.S. Murry, J. Jakowski, J. Simons, *J. Phys. Chem. B* 110 (2006) 14283–14291.
- [20] Y. Romero, F. Richard, S. Brunet, *Appl. Catal. B* 98 (2010) 213–223.
- [21] M.J. Girgis, B.C. Gates, *Ind. Eng. Chem. Res.* 30 (1991) 2021–2058.
- [22] A.G. Gayubo, A.T. Aguayo, A. Atutxa, R. Aguado, M. Olazar, J. Bilbao, *Ind. Eng. Chem. Res.* 43 (2004) 2619–2626.
- [23] A.G. Gayubo, A.T. Aguayo, A. Atutxa, R. Aguado, J. Bilbao, *Ind. Eng. Chem. Res.* 43 (2004) 2610–2618.
- [24] P.D. Chantal, S. Kaliaguine, J.L. Grandmaison, *Appl. Catal.* 18 (1985) 133–145.
- [25] P.A. Horne, P.T. Williams, *Renew. Energy* 7 (1996) 131–144.
- [26] J.D. Adjaye, N.N. Bakhshi, *Fuel Process. Technol.* 45 (1995) 185–202.
- [27] J.D. Adjaye, N.N. Bakhshi, *Biomass Bioenergy* 8 (1995) 131–149.
- [28] X.L. Zhu, R.G. Mallinson, D.E. Resasco, *Appl. Catal. A* 279 (2010) 181.
- [29] C.D. Chang, A.J. Silvestri, *J. Catal.* 47 (1977) 249.
- [30] X.L. Zhu, L.L. Lobban, R.G. Mallinson, D.E. Resasco, *J. Catal.* 271 (2010) 88–98.
- [31] T.Q. Hoang, X.L. Zhu, T. Sooknoi, D.E. Resasco, R.G. Mallinson, *J. Catal.* 271 (2010) 201–208.
- [32] C. Zhao, Y. Kou, A.A. Lemonidou, X.B. Li, J.A. Lercher, *Angew. Chem. Int. Ed.* 48 (2009) 3987–3990.
- [33] C. Zhao, Y. Kou, A.A. Lemonidou, X.B. Li, J.A. Lercher, *Chem. Commun.* 46 (2010) 412–414.
- [34] D.Y. Hong, S.J. Miller, P.K. Agrawal, C.W. Jones, *Chem. Commun.* 46 (2010) 1038–1040.
- [35] C.A. Fisk, T. Morgan, Y.Y. Ji, M. Crocker, C. Crofcheck, S.A. Lewis, *Appl. Catal. A* 358 (2009).
- [36] A. Gutierrez, R.K. Kaila, M.L. Honkela, R. Slioor, A.O.I. Krause, *Catal. Today* 147 (2009) 239–246.
- [37] J.Q. Bond, D.M. Alonso, D. Wang, R.M. West, J.A. Dumesic, *Science* 327 (2010) 1110–1114.
- [38] W.E. Farneth, R.J. Gorte, *Chem. Rev.* 95 (1995) 615–635.
- [39] T.J.G. Kofke, R.J. Gorte, G.T. Kokotailo, W.E. Farneth, *J. Catal.* 115 (1989) 265–272.
- [40] Y. Takagi, S. Nishimura, K. Taya, K. Hirota, *J. Catal.* 8 (1967) 100–104.
- [41] P.E. Ruiz, K. Leiva, R. Garcia, P. Reyes, J.L.G. Fierro, N. Escalona, *Appl. Catal. A* 348 (2010) 78–83.
- [42] A. Popov, E. Kondratieva, J.M. Goupil, L. Marley, P. Bazin, J.P. Gilson, A. Travert, F. Mauge, *J. Phys. Chem. C* 114 (2010) 15661–15670.